

# We are IntechOpen, the world's leading publisher of Open Access books Built by scientists, for scientists

**4,800**

Open access books available

**122,000**

International authors and editors

**135M**

Downloads

Our authors are among the

**154**

Countries delivered to

**TOP 1%**

most cited scientists

**12.2%**

Contributors from top 500 universities



**WEB OF SCIENCE™**

Selection of our books indexed in the Book Citation Index  
in Web of Science™ Core Collection (BKCI)

Interested in publishing with us?  
Contact [book.department@intechopen.com](mailto:book.department@intechopen.com)

Numbers displayed above are based on latest data collected.

For more information visit [www.intechopen.com](http://www.intechopen.com)



---

# High Accuracy Calibration Technology of UV Standard Detector

---

Wang Rui, Wang Tingfeng, Sun Tao, Chen Fei and Guo Jin

Additional information is available at the end of the chapter

<http://dx.doi.org/10.5772/48344>

---

## 1. Introduction

Nowadays, with the development of the technology, Ultraviolet optics has showed great implication prospect in the fields of space science, material, biophysics and plasma physics. Recently, with the development of the space remote sensing, the UV remote sensing technology has been re-known. The atmosphere is not only the main carrier and activity stage of earth climate and environment, but also is the main element of the space circumstance. So, realizing the global uniform sensing, always has been the common object of earth and space science community.

UV remote sensing is a necessary method of knowing the vertical structure and change of the atmosphere intensity<sup>[1]</sup>, Ozone, gasoloid, and monitoring the state and turbulence of the middle layer atmosphere. It has a great science meaning in knowing the interacting procedure between the upper and lower atmosphere, establishing and proving the dynamic atmosphere model, and understanding the relationship between the sun activity and the climate of the space and earth.

With the developing of the quantization remote sensing researching, and the increasing of the test accuracy. All kinds of sensors have to be calibrated by the high accuracy standard at UV wavelength, and the testing accuracy, long-time stability and the date comparative of the sensors have to be evaluated. In theory, there are two way in realizing the absolute radiation calibration, the first one is standard light calibration method, and the second one is standard detector calibration method. The standard light calibration method is so easy to realizing the standard transmitting in the whole wavelength, but some uncertainty factor has also been introduced, it makes the calibration accuracy increasing so hardly. Because the uncertainty of the standard source is so low(1.2%), and some method has been using in removing a lot of uncertainty factor, the standard detector calibration method would been a effective way in increasing the calibration accuracy at UV wavelength. This section will have

a discussion about the UV detector calibration method, analyzing the calibration theory, establishing the experiment system, and finally gives a complete high accuracy UV standard detector calibration method.

## 2. UV detector standard and standard transmission

### 2.1. Present status and development of the cryogenic radiometer

First of all, the source of the UV detector standard will be introduced. Nowadays, the cryogenic radiometer had been used as the UV absolute standard detector in the world. The cryogenic radiometer is developed on the basic of the cold radiometer. The cold radiometer is the earliest detector which applying as the radiation measurement reference. There is a layer of black material with high absorptance on the receive area of the cold radiometer, the receive area would have a temperature rising when receiving the light. Using the equivalence between the electric heating and the light heating to testing the radiation power is the working principle of the cold radiometer. The cold radiometer has went through several generation development, until the 1980s, the uncertainty of using the cold radiometer to test the radiation power is about 0.1%. Because the cold radiometer working at the normal temperature, and affecting by the material and environment. the testing uncertainty can't been reduced.

In the middle of the 1980s, J.Martin made the fist cryogenic radiometer [2]. It has the same working principle with the cold radiometer. Because working at the liquid temperature, the cryogenic radiometer gets rid of the limitation of the environment and material. The uncertainty had been reduced by an order. So the great performance displayed by the cryogenic radiometer brought the researching on the cryogenic radiometer technology by the measurement organization in the industry development countries. The cryogenic radiometer technology is also hot point and focal point in the field of the radiation measurement now. In 1996, the international measurement organization made a cryogenic radiometer comparison. There are 16 nation measurement organizations joining the comparison. The comparison result indicated that the testing uniformity of each country was about  $3 \times 10^{-4}$ . This is the best comparison result of the international comparing. So the cryogenic radiometer has been the highest accuracy radiation measurement method in the world.

### 2.2. The system structure and working principle of the cryogenic radiometer

The system structure and working principle of the US.NIST (National Institute of Standards and Technology) HARC (high-accuracy cryogenic radiometer) would be introduced as an example. Cryogenic radiometers provide an absolute basis for optical power (flux) measurements at the lowest possible uncertainties. They are used as primary standards for optical power at many other national laboratories as well [3-8]. A cryogenic radiometer is an electrical substitution radiometer (ESR) that operates by comparing the temperature rise induced by optical power absorbed in a black receiving cavity to the electrical power needed to cause the same temperature rise by resistive (ohmic) heating. Thus the measurement of

optical power is determined in terms of electrical power, watt, via voltage and resistance standards maintained by NIST. There are several advantages to operating at cryogenic temperatures ( $\approx 5$  K) instead of room temperature. The heat capacity of copper is reduced by a factor of 1000, thus allowing the use of a relatively large cavity. Also the thermal radiation emitted by the cavity or absorbed from the surroundings is reduced by a factor of  $\approx 10^7$ , which eliminates radiative effects on the equilibrium temperature of the cavity. Finally, the cryogenic temperature allows the use of superconducting wires to the heater, thereby removing the nonequivalence of optical and electrical heating resulting from heat dissipated in the wires. Consequently, most electrical substitution radiometers, including NIST-maintained ESRs, operate at cryogenic temperatures.

The Optical Technology Division within NIST presently has two cryogenic radiometers that provide the basis for the spectral radiant power responsivity scale: the NIST-designed POWR (Figure 1), and the L-1 ACR<sup>[9]</sup> (Figure 2). The POWR is the primary U.S. national standard for the unit of optical power. It has the capability to optimize its configuration for measurements in different spectral regions and for different input laser power levels. For optimized noise performance, it can operate at temperatures as low as 1.7 K for extended periods. The L-1 ACR is also an absolute radiometer, but one whose operation is optimized for the  $\mu\text{W}$  to mW power levels in the UV to NIR spectral region. In comparison with POWR, the L-1 ACR is compact and mobile, which makes it a convenient instrument to use for scale transfers. The relative combined standard uncertainty of the NIST cryogenic radiometer measurements range is from 0.01 % to 0.02 % in the visible region of the spectrum<sup>[10]</sup>. The largest components of the uncertainty are those due to the systematic correction for the Brewster angle window transmittance and the nonequivalence between electrical and optical heating. A comparison between POWR and the L-1 ACR showed that these two standards agreed to within 0.02 %, which is within their combined uncertainties as shown in Figure 3<sup>[9]</sup>.

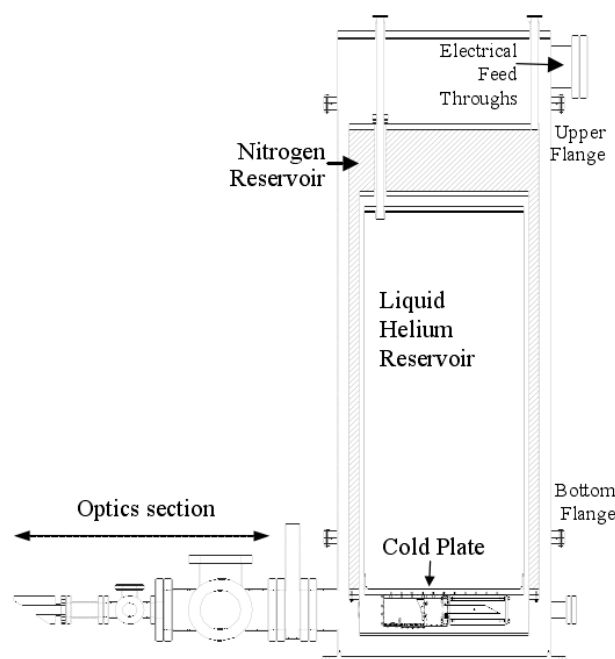


**Figure 1.** The construction of the NIST Primary Optical Watt Radiometer(POWR)

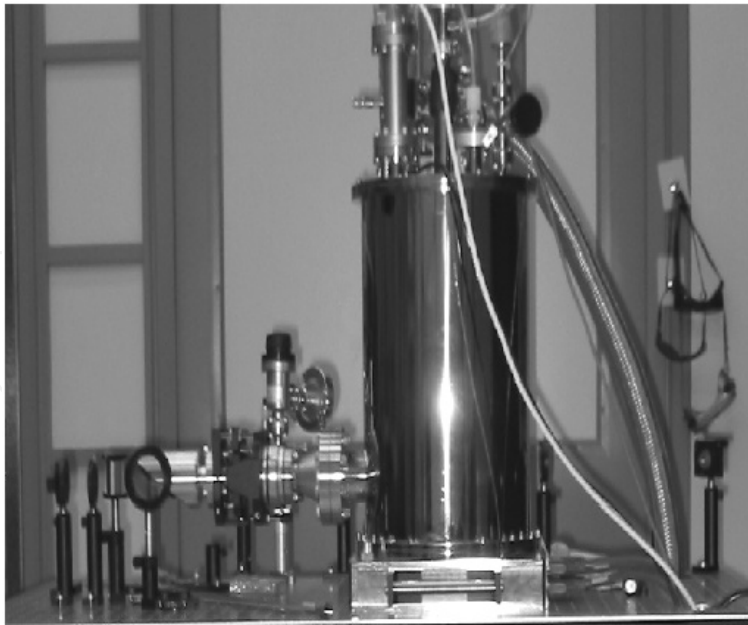


**Figure 2.** The NIST L-1 ACR used in Spectral Irradiance and Radiance Responsivity Calibrations using Uniform Sources (SIRCUS)

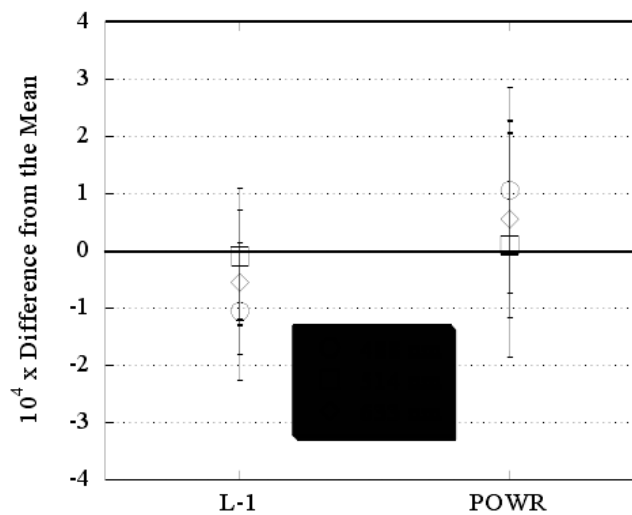


**Figure 3.** Comparison of POWR and the L-1 ACR measurements showing the agreement between the ACRs. The error bars are the measurement uncertainty

## 2.3. The procedure of the detector standard transmitting

### 2.3.1. Calibration of transfer standards with a cryogenic radiometer

The NIST detector standard transmitting procedure will be discussed as an example. The cryogenic radiometers described above use lasers as their source and a variety of transfer detectors to disseminate the spectral power responsivity scale. Historically, the scale was realized using the High Accuracy Cryogenic Radiometer (HACR) <sup>[11]</sup> at nine discrete laser lines in the visible wavelength range. A physical model was developed to interpolate the responsivity of silicon trap detectors over the spectral range from 405 nm to 920 nm <sup>[12]</sup>.

Outside of this spectral range, the detector responsivity scale was based on pyroelectric detector with a spectrally flat responsivity [13]. While the pyroelectric detector had a spectrally flat responsivity, its absolute responsivity value was low. While it could extend the scale, its noise performance dramatically increased the uncertainties in the UV and the NIR spectral regions because of the low flux available on the comparator facilities (see the 1998 version of this document [14] for more information). The UV responsivity scale uncertainty was improved by calibrating the UV WS (UV working standard) at the NIST Synchrotron Ultraviolet Radiation Facility (SURF III) with an ACR-monochromator system [15, 16].

### 2.3.2. Calibration of the working standards

Two UV working standards (UV WS) were calibrated from 200 nm to 400 nm by a series of measurements at the Ultraviolet Spectral Comparator Facility (UV SCF), Visible to Near-Infrared Spectral Comparator Facility (Vis/NIR SCF), and SURF with various Si photodiode UV transfer standards and trap detectors. The UV WS were calibrated with a Vis Trap at the Vis/NIR SCF from 405 nm to 500 nm. The combination of the UV transfer standards and the Vis Trap provides the lowest uncertainties over the entire UV WS calibration range. The calibration chain for the UV working standards is shown in Figure 4.

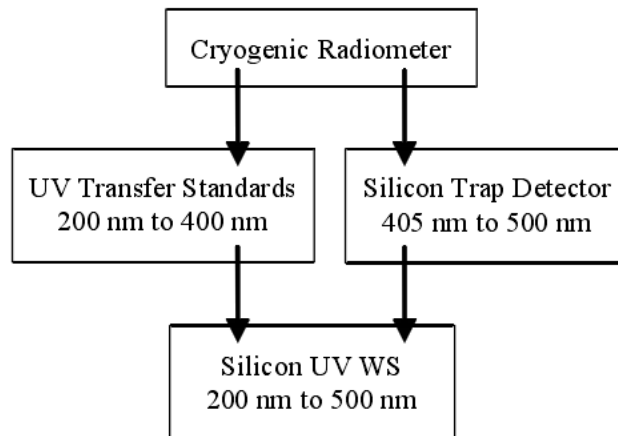


**Figure 4.** The calibration chain for the ultraviolet working standards (UV WS)

The responsivity of the UV WS was determined by an average of 3 independent scans against each UV TS and Vis Trap. As with the Vis WS, each UV WS was removed from the SCF and realigned between each scan. The resulting data from the transfer standards were combined to create a single scale from 200 nm to 500 nm for the UV WS.

### 2.3.3. Ultraviolet Spectral Comparator (UV SCF)

The UV SCF is a monochromator-based system that measures the uniformity and spectral power responsivity of photodetectors in the 200 nm to 500 nm spectral region. The UV SCF is very similar in configuration and operation to the Vis/NIR SCF. Only the differences between the two will be described. A diagram of the UV SCF is shown in Fig. 5

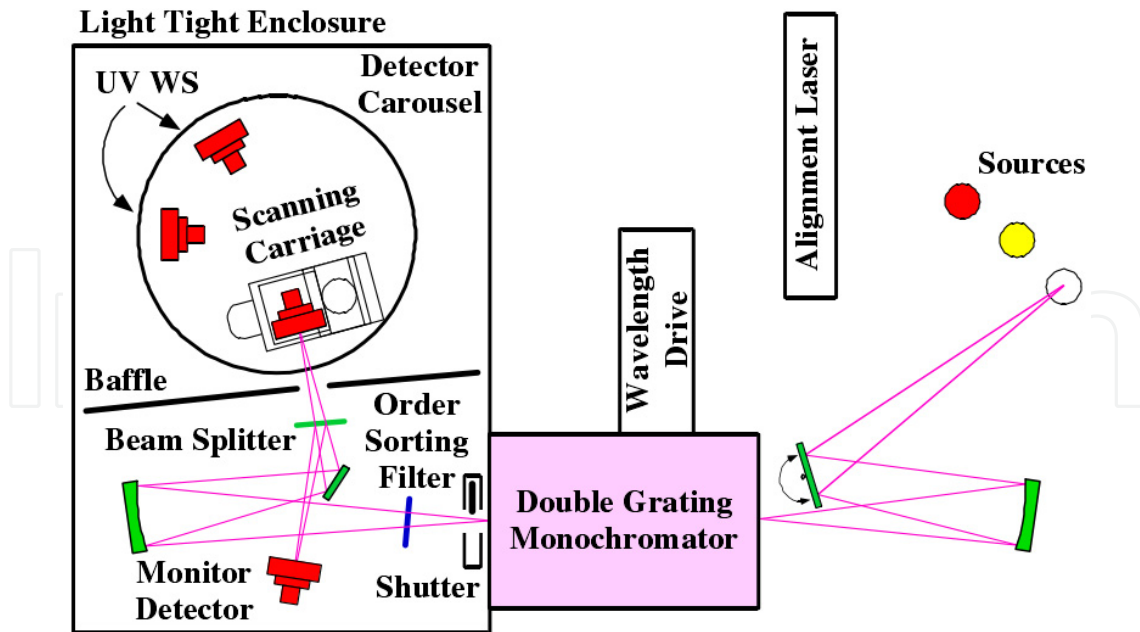


**Figure 5.** Ultraviolet Spectral Comparator Facility (UV SCF)

UV enhanced silicon photodiodes serve as the working standards for the UV SCF. A rotary stage is used in the UV SCF; currently only one test detector at a time can be measured. The test and working standard detectors are fixed onto optical mounts that rotate and tilt. Motorized translation stages position the test detector in the horizontal and vertical planes while the working standards are positioned manually.

### 3. High Accuracy UV Standard Radiometer (HAUVSR)

As the main radiation testing facility, the radiometer has an important position in the radiation field. But the radiometer used in the practical application doesn't have a responsibility standard, needs to be calibrated by the standard source. Because of the error introduced in the calibration procedure, the radiometer uncertainty will reduce. So the radiometer doesn't have a good performance in the radiation application<sup>[17]</sup>.

For solving the problem discussed above, the HAUVSR had been established using the NIST working standards detector as a core element. A series of capability testing had been made to confirm its stability. And the HAUVSR responsibility standard had been deduced at the basic of the NIST detector standard. The uncertainty analyzing also had been done. Finally, there is a radiometer with high stability, high accuracy and self-responsivity standard that would have a great performance in the calibrating application.

#### 3.1. Establishmen of the HAUVSR

##### 3.1.1. System construction

The design concept of the HAUVSR is compact structure, easy to carrying on, simple interior constitution and stability performance. And there is no other optical element in the HAUVSR. So the responsibility standard can be deduced with high accuracy.

For satisfying the requirement listing above, The HAUVSR has been established using the NIST working standards detector as a core element, and adding the light filter splitting system, motor driving system and data acquisition system. The structure of the whole facility is shown in Fig.6

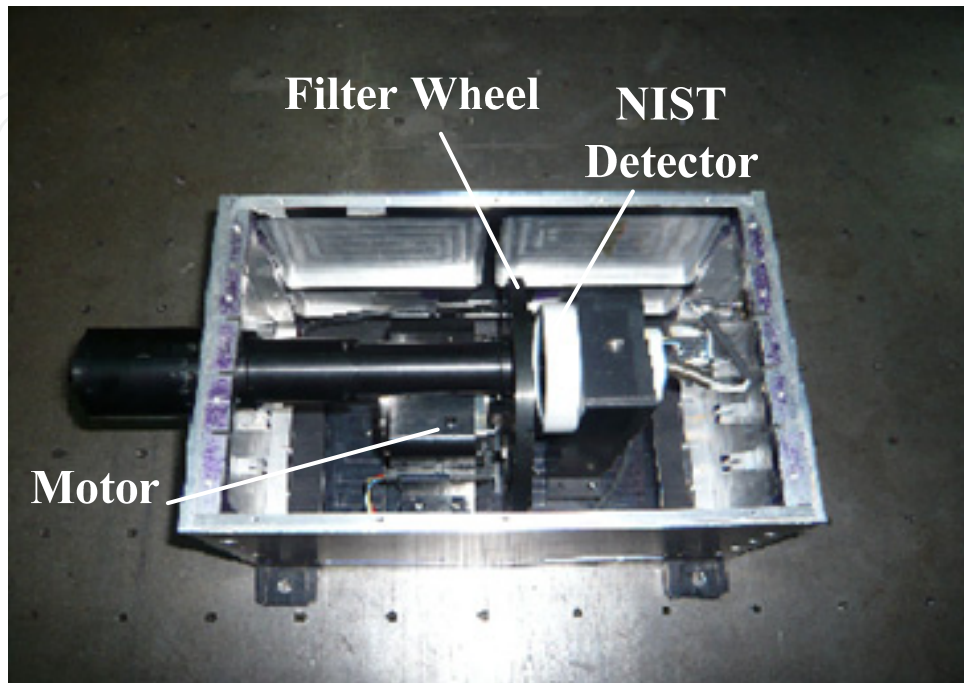


**Figure 6.** The structure of the HAUVSR

The incident light pass through the lightproof canister, filter, and arrives at the receive area of the detector. There is three UV filter with different wavelength fitting on the filter wheel. The three wavelengths are 313nm, 352nm, 365nm. The filter wheel is controlled by the motor driving to make sure different wavelength light passing through. The data acquisition system collects the detector signal and saves it on the computer. According to the responsivity standard of the HAUVSR, the incident optical radiation can be calculated with the data.

### 3.1.2. Detector selection

As the core element of the HAUVSR, The detector's performances will effect the accuracy and stability of the HAUVSR. So the detector choosing is very important. According to the design requirement of the HAUVSR, a detector with good stability, great linearity, compacting structure, wide response wavelength range and self-responsivity will be used standard. After considering all the factor, the NIST working standard detector S2281 will be the best choice. The advantage of the NIST detector will display obviously in a series of testing results by comparing with the HAMAMATSU detector.

#### a. Space Uniformity Testing of Detector Receive Area

Space uniformity is a very important character of Si detector. In theory, the detector would have great space uniformity, it means that the output signal will be sameness, when incident



optical radiation illuminate on the difference zone of the detector receive area. But the uniformity actually is restricted by the photo surface material, making technique and the little speck on the photo surface. And the detector receive area heterogeneity will effect the testing accuracy.

The detector space uniformity testing system is shown in Fig.7. At first, the untested detector would be fitted on the detector rotary table which can move at X and Y direction. The moving distance is 50mm. Two-direction repeatable accuracy  $< 2 \mu\text{m}$ . There are a  $\phi 1\text{mm}$  apertures stop and two lens before the detector. A  $\phi 1\text{mm}$  optical speckle on the receive area can be acquired by secondary imaging. The responsivity with different coordinate can be tested by varying the detector position. The testing wavelength is 350nm. The scanning area is 10mmx10mm with 1mm interval. And the delay time is 5 second.

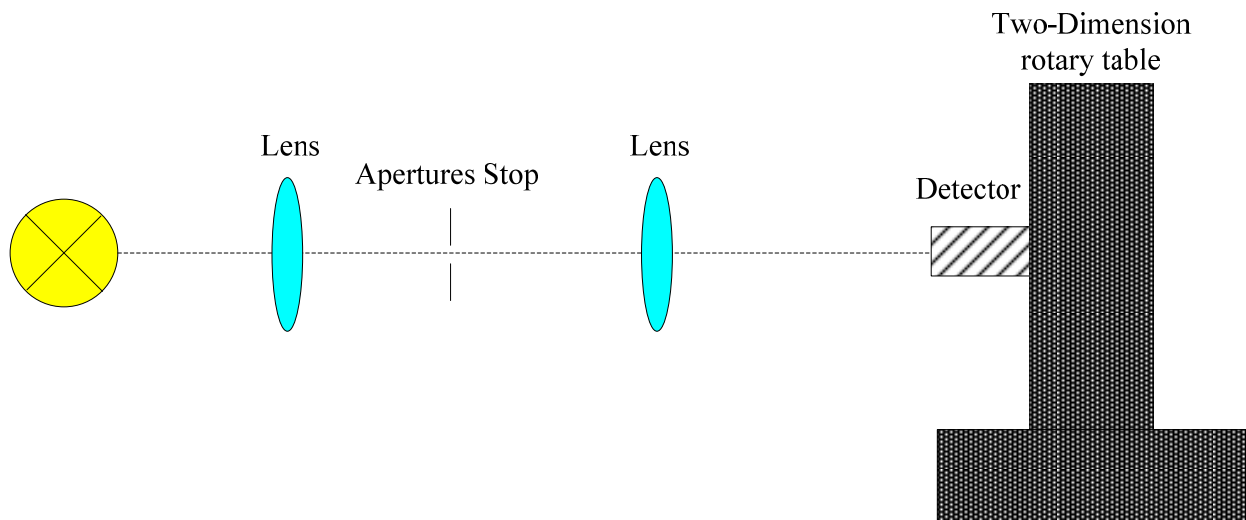


**Figure 7.** Detector Space Uniformity testing system

Three detectors had been tested (NIST S2281 detector and two HAMAMATSU detectors). The testing result (different position responsivity) had been normalized. And the 3D figure had been drawn using the MatLab software. Fig.7 displays the responsivity space uniformity of the three detectors.

Just like shows in Fig.8, the space uniformity of the NIST detector has a great advantage comparing with the two HAMAMATSU detectors. The three detector's space uniformity also can be calculated. The result is shown in Table.1.

Detector	Space Uniformity
The Space Uniformity of NIST S2281 detector	$\leq 1.5\%$
The Space Uniformity of HAMAMATSU detector 1	$\leq 2.7\%$
The Space Uniformity of HAMAMATSU detector 2	$\leq 2.4\%$

**Table 1.** The Space Uniformity of the three Detectors

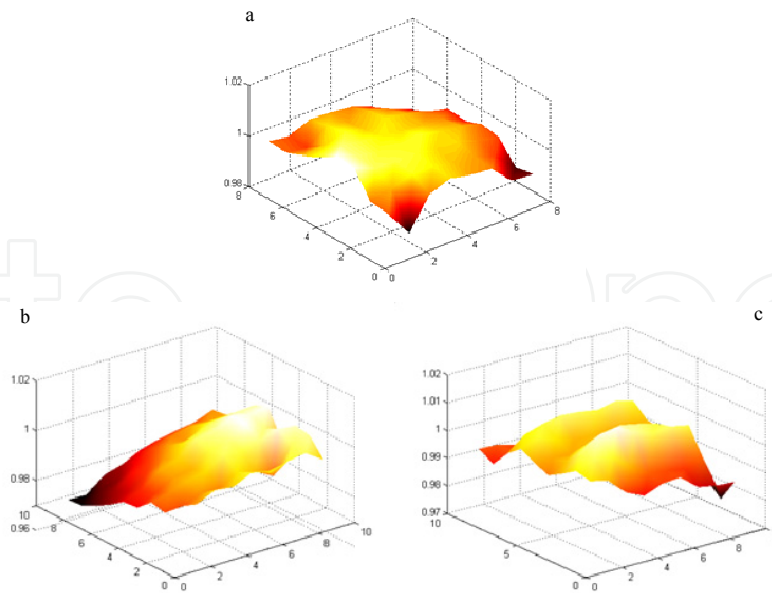


**Figure 8.** Detector Space uniformity curved  
(a.NIST S2281 detector; b. HAMAMATSU detector1; c. HAMAMATSU detector2)

### b. Detector linearity

Linearity is a basic feature of detector. In theory, the detector responsivity is stationary<sup>[18]</sup>. The responsivity won't change when the incident optical power varies.

There are a lot of methods for detector linearity testing, just like inverse ratio method of distance square, polarizing film method and so on. Neutral weakener and double optical stops method with high accuracy had been adopted in this section.

Fig.9 shows the linearity testing facility. The standard light F08 had been used. The detector had been putted into a light-tight box to eliminating the stray light. The neutral weakener was fitted on the filter wheel, and putted before the detector. Double light stop is laid between the light and the weakener. Different neutral weakener was moved into the light path by controlling the filter wheel to realize the incident optical energy varying. The weakener gradient is 0.01%, 0.1%, 1%, 10%, 31.62%, 50.12%, 79.43%, 100%. And the signal with different optical stop would be saved.

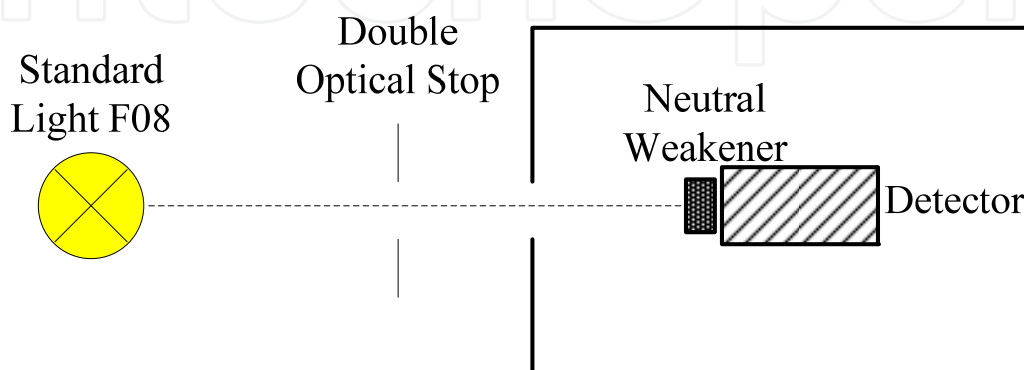


**Figure 9.** Detector Linearity testing facility

The testing results shows that the NIST detector linearity is about 0.6% in the  $10^4$  dynamic ranges, and the HAMAMATSU linearity is about 0.7%. So the NIST detector linearity can satisfy the design requirement of the HAUVSR.

### 3.1.3. The filter stability and uniformity testing

According to the design requirement of the HAUVSR, the filter needs to own some characteristic listing below:

1. Narrow band width : Narrow band width is propitious to calculate the self-responsivity of the HAUVSR.
2. High stability: The stability of the filter will effect the HAUVSR performance.
3. Great uniformity: The filter's transmittance uniformity will have a influence on the HAUCSR testing accuracy.

So some filters which produced by different manufactory had been tested. Finally, some filter which could satisfy the requirement had been selected.

The filter stability had been tested for 1 year. The test result is shown in Table.2

Filter	Central Wavelength		
	2008.6	2009.6	changes
280.000	280.150	280.250	0.100
313.000	314.300	314.450	0.150
352.000	353.500	353.350	0.015
365.000	364.950	364.750	0.020
Filter	Band Width		
	2008.6	2009.6	changes
280.000	25.500	24.300	1.200
313.000	10.600	9.800	1.100
352.000	10.100	8.900	1.200
365.000	11.400	10.400	1.000
Filter	Peak Transmittance		
	2008.6	2009.6	changes
280.000	0.277	0.271	0.006
313.000	0.648	0.643	0.002
352.000	0.551	0.549	0.002
365.000	0.438	0.432	0.006

**Table 2.** Filter Long Time Stability Testing

The testing result showed that the central wavelength, band width, peak transmittance of the filter had so little change in a year to satisfy the design requirement.

For limiting by the facture technics the filter transmittance uniformity had a discrepancy. The filter uniformity had been tested with the testing facility introduced in the section 3.1.2.

There are 9 points being selected to do the test. The diameter of the optical speckle is 1mm. Just like shows in Fig.10.

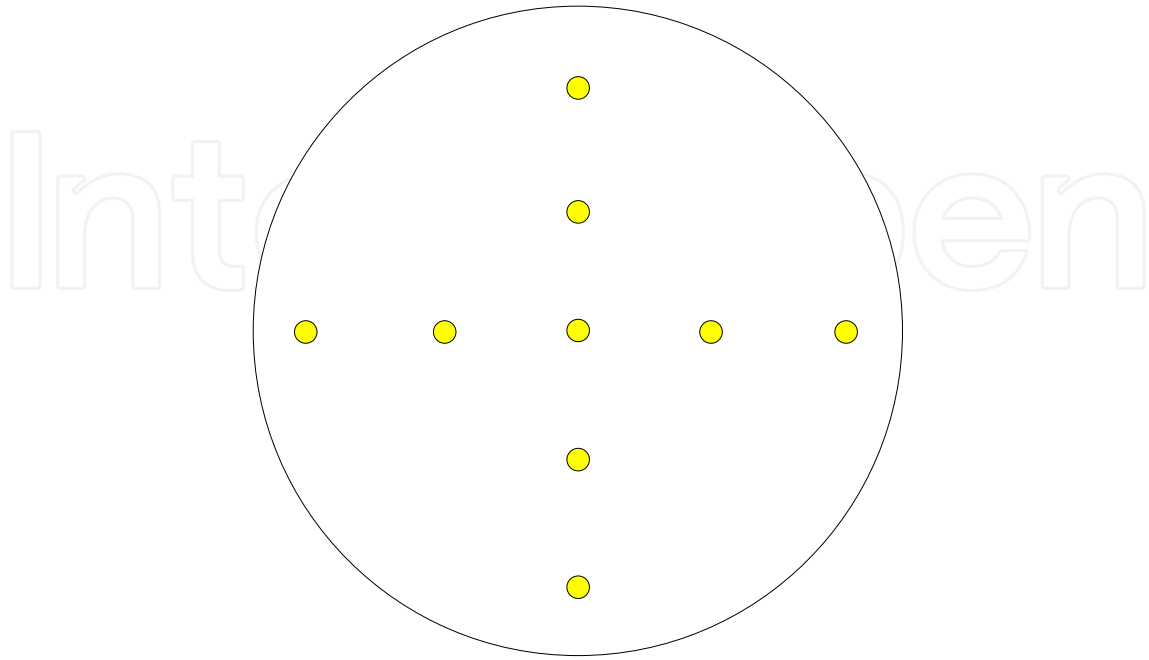


**Figure 10.** Filter Transmittance Uniformity Testing

The testing result shows in Table.3

Filter	Nonuniformity
280.000	0.06%
313.000	0.05%
352.000	0.07%
365.000	0.04%

**Table 3.** The Testing Result of the Filter Transmittance Uniformity

The testing result displays that the filter transmittance uniformity is so great that its influence on the HAUVSR could be ignored.

### 3.2. High Accuracy UV Standard Radiometer performance testing

The whole HAUVSR system had been tested on the basic of performance evaluation of the core elements.

The output signal from the HAUVSR would effect the testing accuracy. So it is so necessary to test the HAUVSR signal repeatability <sup>[19]</sup>.

Using the standard light F08 with stable output, the signal form HAUVSR had been tested for 20 times at 3 wavelengths in 3 months. After standard deviation calculate with the data. The signal repeatability result is shown in Fig.11. The signal standard deviation is less than 0.6% at three wavelengths.

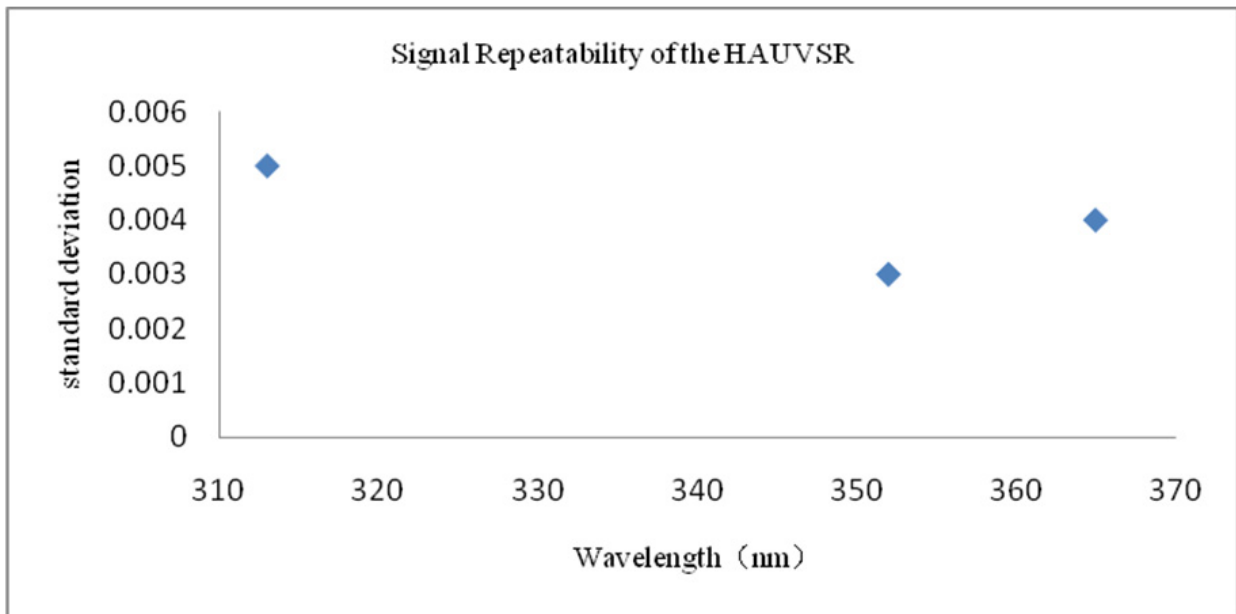


**Figure 11.** Signal Repeatability of the HAUVSR

The signal repeatability had also been tested in different temperature. The varying range of the temperature is 15<sup>0</sup>C-32<sup>0</sup>C. The testing result shows in Fig.12. The testing result had proved the great stability of the HAUVSR.

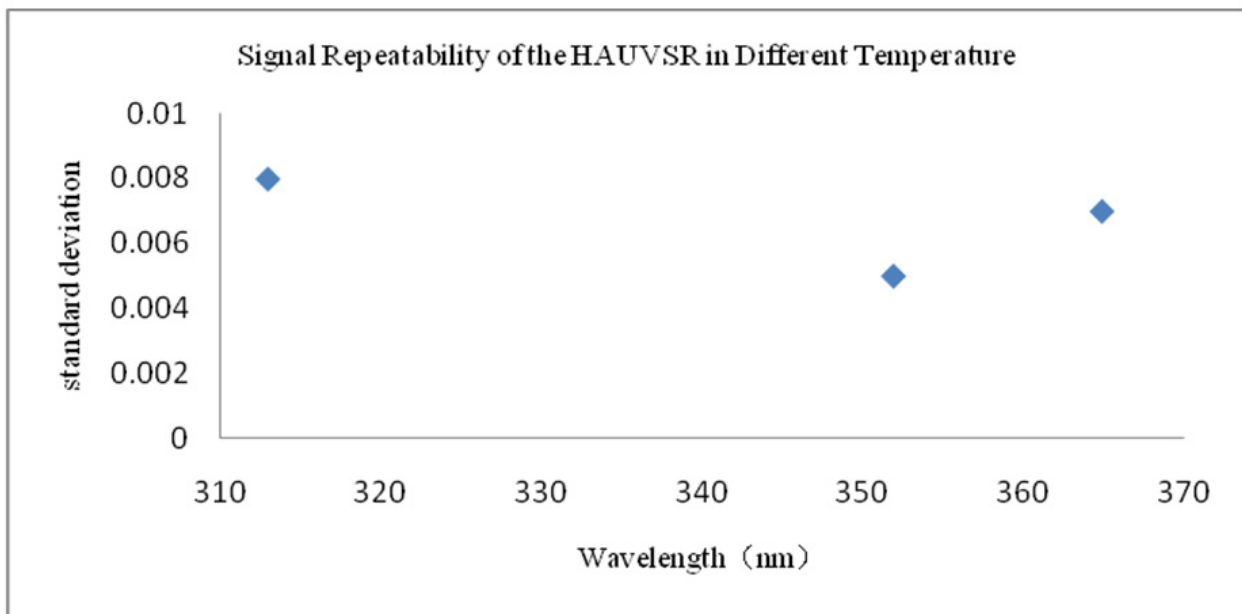


**Figure 12.** Signal Repeatability of the HAUVSR in Different Temperature

### 3.3. The responsivity deducing of the high accuracy UV radiometer

As the core element of the HAUVSR, the NIST working standards detector’s spectral responsivity had been calibrated in NIST. The calibration procedure had been introduced in the section 2.3. But the calibration result is the radiant flux responsivity, and the irradiance

and radiance responsivity always are used in application. So the HAUVSR irradiance and radiance responsivity had to be deduced in this section.

### 3.3.1. Irradiance and radiance responsivity deducing of the HAUVSR

First of all, the definition of the radiant flux, irradiance and radiance is given.

The radiant flux  $\Phi$  is given by:

$$\Phi = \frac{dQ}{dt} \quad (1)$$

$dQ$  is the transmission and receiving radiation energy in the time of  $dt$

The irradiance that is the illuminated radiant flux at unit surface can be written as:

$$E = \frac{d\Phi}{dA} \quad (2)$$

And the radiance  $L$  can be written as:

$$L = \frac{d\Phi}{d\Omega dA \cos\theta} \quad (3)$$

$dA$  is the unit radiant surface,  $d\Omega$  is the unit spatial angle,  $\theta$  is the separation angle between the radiant direction and the surface normal direction.

The responsivity  $R$  defines as the electric signal generating by the unit radiant quantity.

1. Radiant flux responsivity

$$R_{\phi} = S / \phi \quad (4)$$

2. Irradiance responsivity

$$R_E = S / E \quad (5)$$

3. Radiance responsivity

$$R_L = S / L \quad (6)$$

$S$  is the system output signal,  $E$  is the irradiance receiving by the system, and  $L$  is the radiance receiving by the system.

According to the Ep.(2) and Ep.(5), the  $R_E$  also can be written as :

$$R_E = R_{\phi} \cdot dA \quad (7)$$

So the irradiance responsivity is given as Ep.(8) according to the Ep.(3) and Ep.(6),

$$R_L = R_\phi \cdot d\Omega \cdot dA \cdot \cos\theta \quad (8)$$

### 3.3.2. Radiant energy proportionality coefficient deducing in the filter band width

There are three filters in the HAUVSR. The band width and peak transmittance of the filters will effect the spectral responsivity of the HAUVSR. So the filter modifying factor has to be added in the responsivity deducing procedure.

The band width of the filters being used are 10.6nm, 10.1nm and 11.4nm. But the calibration data band width of the NIST working standards detector is 1nm after interpolation calculating. The radiant energy transmission proportionality coefficient in narrow band width will be deduced in this section.

At first, the transmissivity of the filters has to be tested with spectrometer Lamda950. The wavelength interval is 0.5nm.  $T(\lambda)$  is the transmissivity at different wavelength.  $I(\lambda)$  is the incident radiant energy.  $R(\lambda)$  is the detector responsivity. So the optical radiation receiving by the detector can be written in general:

$$I_d = \int_{\lambda_1}^{\lambda_2} I(\lambda) \cdot T(\lambda) \quad (9)$$

The detector output signal  $S_d$  is:

$$S_d = \int_{\lambda_1}^{\lambda_2} I(\lambda) \cdot T(\lambda) \cdot R(\lambda) \quad (10)$$

$S_m$  is the signal at central wavelength, it can be written as:

$$S_m = I(\lambda_m) \cdot T(\lambda_m) \cdot R(\lambda_m) \quad (11)$$

So the proportionality coefficient in narrow band width  $f$  can be obtained through dividing Ep.(11) by Ep.(10):

$$f = \frac{S_m}{S_d} = \frac{I(\lambda_m) \cdot T(\lambda_m) \cdot R(\lambda_m)}{\int_{\lambda_1}^{\lambda_2} I(\lambda) \cdot T(\lambda) \cdot R(\lambda)} \quad (12)$$

### 3.3.3. The correction factor deducing of detector uniformity

As the optical radiation receiving instrument, the detector uniformity will effect the HAUVSR testing accuracy. So the correction factor of detector uniformity has to be added in the process of the HAUVSR responsivity deducing.

According to the detector uniformity testing result in the section 3.1.3, the detector nonuniformity normalization value  $B_i$  can be obtained. The nonuniformity correction factor can be written as:

$$\gamma = \frac{\int_1^m B_i R}{mR} = \frac{\int_1^m B_i}{m} \quad (13)$$

### 3.3.4. The HAUVSR responsivity deducing result

According to the correction factors discussing above, the HAUVSR spectral responsivity is:

1. HAUVSR irradiance responsivity :

$$R_E = \frac{R_\phi \cdot \gamma \cdot A \cdot \tau}{f} \quad (14)$$

2. HAUVSR radiance responsivity :

$$R_L = \frac{R_\phi \cdot \Omega \cdot \gamma \cdot A \cdot \tau}{f} \quad (15)$$

### 3.3.5. The uncertainty of the HAUVSR

According to the Ep.(14) and Ep.(15) , the uncertainty of the HAUVSR can be written as:

$$\frac{\Delta R_s(\lambda)}{R_s(\lambda)} = \left\{ \left| \frac{\Delta R_\phi(\lambda)}{R_\phi(\lambda)} \right|^2 + \left| \frac{\Delta \gamma(\lambda)}{\gamma(\lambda)} \right|^2 + \left| \frac{\Delta f(\lambda)}{f(\lambda)} \right|^2 + \left| \frac{\Delta \tau(\lambda)}{\tau(\lambda)} \right|^2 \right\}^{1/2} \quad (16)$$

The uncertainty item are listed in the Table.4

Uncertainty Source	value
The NIST detector uncertainty	1.1%
The testing and calculating error of the correction factor $\gamma$	0.5%
The testing and calculating error of the correction factor $f$	0.5%
The testing correction of filter transmissivity $\tau$	0.5%
The stray light uncertainty	0.3%
Total uncertainty	1.3%

**Table 4.** The uncertainty of the HAUVSR

1. The NIST standard detector uncertainty 1.1% is given by NIST calibration result.
2. The uncertainty of the detector uniformity correction factor  $\gamma$  is decided by the number of the testing point and the instrument accuracy. The uncertainty value is 0.3%



3. The uncertainty of the correction factor  $f$  is also decided by the testing and calculating error. The value is 0.3%.
4. The uncertainty of the filter transmissivity  $\tau$  is effected by the Lamda950 testing error. The value is 0.5%.

#### 4. The untested spectrometer responsivity calibrated with standard detector calibration method

After a series of deducing in the section 3.3, the HAUVSR had self- responsivity standard. So the HAUVSR can be used to calibrate the untested sensor with standard detector calibration method. The basic theory of standard detector calibration method is that the responsivity of untested sensor can be acquired when the two device receive the same incident optical radiation. Because the responsivity of standard detector is known, the untested sensor calibration result can be obtained easily with substitution method<sup>[20]</sup>.

In this section, The HAUVSR system will be used as a standard detector to calibrate the untested spectrometer with standard detector calibration method.

##### 4.1. Irradiance responsivity calibration with standard detector calibration method

The calibration instrument is shown in Fig.13. A quartz tungsten-halogen lamp with great stability is used. The HAUVSR and untested spectrometer are putted on the experiment table. The distance between the HAUVSR and the lamp is 650mm<sup>[21]</sup>. The lamp center and the optical stop center of the HAUVSR are fitted at the same horizontal line. The system has to be preheated for 40 minutes before the signal acquisition. There are 3 wavelengths (313nm, 352nm, 365nm) being tested. The signal has to be acquired for 3 times, and calculate an average value to eliminate the random error. Then, the untested spectrometer is moved into the optical path. Keeping the distance of 650mm, the signal is acquired at the same 3 wavelength.

The spectral irradiance receiving by the HAUVSR and the untested spectrometer comes from the same lamp. If the distance between the lamp and sensor is fixed, and the lamp has a great stability, the Ep. (17) can be obtained.  $E_{F08}$  is the spectral irradiance of the quartz tungsten-halogen lamp at the distance of 650mm.  $S_{ES}$ ,  $S_{ED}$  are the signal value of the HAUVSR and the untested spectrometer.  $R_{ES}$ ,  $R_{ED}$  are the irradiance responsivity of the HAUVR and the untested spectrometer.

$$E_{F08} = \frac{S_{ES}}{R_{ES}} = \frac{S_{ED}}{R_{ED}} \quad (17)$$

Because the irradiance responsivity is known, the irradiance responsivity of the untested spectrometer is<sup>[22]</sup>:

$$R_{ED} = \frac{S_{ED} \cdot R_{ES}}{S_{ES}} \tag{18}$$

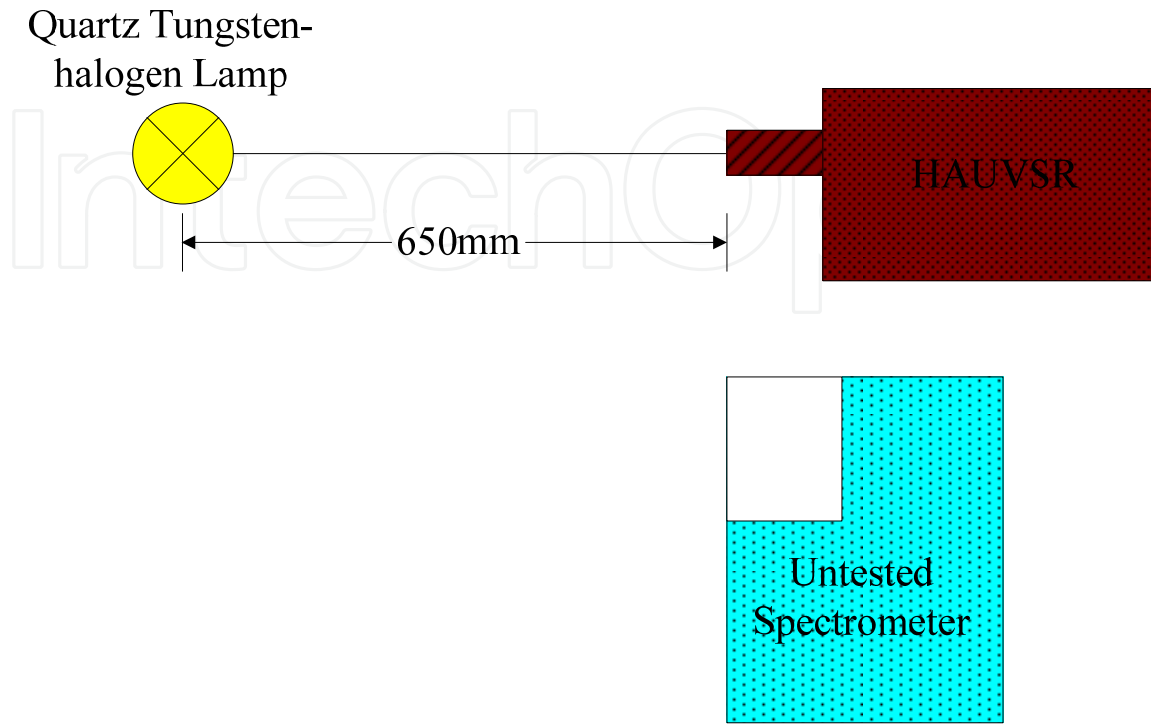


**Figure 13.** The Irradiance responsivity calibration instrument using standard detector calibration method

Substituting the signal measurement into the Ep. (18), the irradiance responsivity of the untested spectrometer  $R_{ED}$  can be acquired.

The uncertainty analyzing can be done with the Ep. (18).

$$\frac{\Delta R_{ED}(\lambda)}{R_{ED}(\lambda)} = \left[ \left| \frac{\Delta S_{ED}(\lambda)}{S_{ED}(\lambda)} \right|^2 + \left| \frac{\Delta R_{ES}(\lambda)}{R_{ES}(\lambda)} \right|^2 + \left| \frac{2\Delta h}{h} \right|^2 \right]^{1/2} \tag{19}$$

The uncertainty item is shown in Table.5

Uncertainty source	Value
The HAUVSR self- responsivity uncertainty	1.3%
The testing error of the distance between the lamp and the instrument	1.2%
The uncertainty generated by the instrument position deviation	0.5%
The wavelength accuracy and repeatability of the untested spectrometer	0.6%
The detecting system excursion and linearly of the untested spectrometer	0.5%
The stray light uncertainty	0.3%
Total uncertainty	1.9 %

**Table 5.** The uncertainty of the standard detector irradiance calibration method

1. The uncertainty of the HAUVSR self- responsivity is 1.3% .(in sec.3.3.5)
2. The testing error of the distance between the lamp and the instrument is about 3mm. using Ep.(19),the uncertainty can be calculated. The value is 1.2%
3. The instrument position deviation will change the separation angle between the untested spectrometer diffused plate and the lamp, and effects the bi-directional reflectivity. The value is 0.5%.
4. The detecting system excursion and linearly of the untested spectrometer is effected by the performance of the amplifier of the detector. The value is about 0.5%.
5. The stray light effect is an assignable factor in the process of calibration. Some measures had been adopted. The experiment table had been masked with black cloth. So there is no obstacle and reflect light around the lamp. The HAUVSR and untested spectrometer has been made black finish. Their surface emissivity is about 0.8%. The measures listing above can minimize the stray light error to 0.3%.

So the uncertainty of the HAUVSR calibrating the untested spectrometer with standard detector method is 1.9%.

#### 4.2. Irradiance responsivity calibration standard light calibration method

Using NIST standard light F528 to calibrate the irradiance responsivity of the untested spectrometer with standard light calibration method is also been done.

The standard light is used to illuminate the center of the diffused plate of the untested spectrometer. The distance between them is 650mm. The calibration instrument is shown in Fig.14.Because the irradiance of the lamp is known, the irradiance responsivity of the untested spectrometer can be obtain easily after getting the output signal.  $E_{F528}$  is the irradiance of the standard light F528.

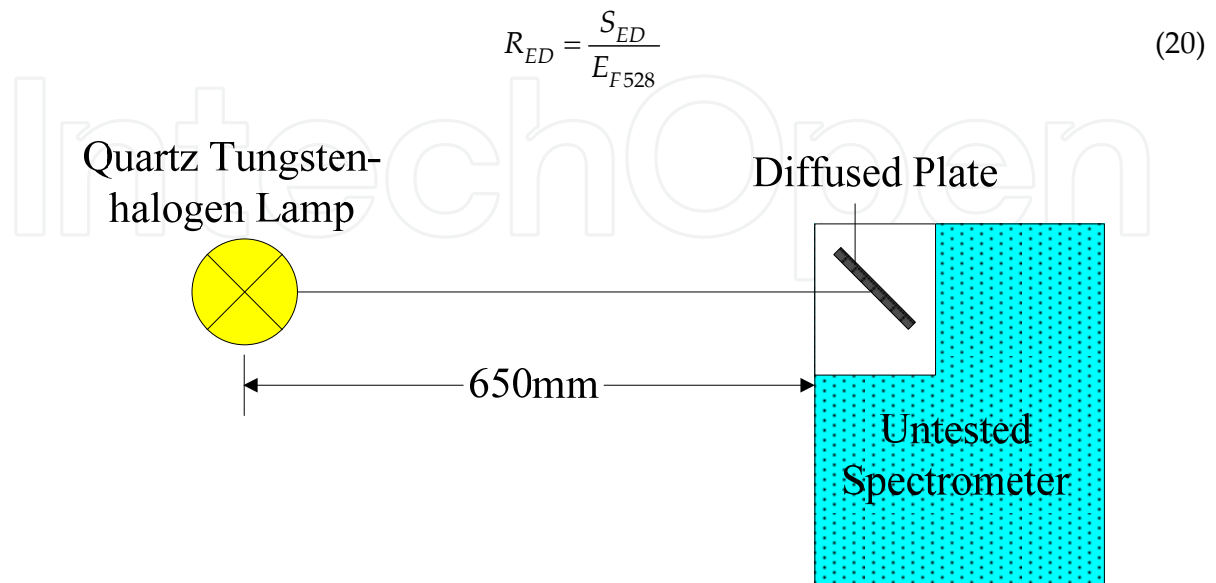


**Figure 14.** The Irradiance responsivity calibration instrument using standard light calibration method

According to the Ep. (20), the uncertainty becomes:

$$\frac{\Delta R_E(\lambda)}{R_E(\lambda)} = \left[ \left| \frac{\Delta S_{ED}(\lambda)}{S_{ED}(\lambda)} \right|^2 + \left| \frac{\Delta E_{F528}(\lambda)}{E_{F528}(\lambda)} \right|^2 + \left| \frac{2\Delta h}{h} \right|^2 \right]^{1/2} \quad (21)$$

The uncertainty item is listed in the Table.6

Uncertainty source	Value
The irradiance uncertainty of the standard light F528	2%
The testing error of the distance $h$ between the lamp and the instrument	1.2%
The uncertainty generated by the instrument position deviation	0.5%
The wavelength accuracy and repeatability of the untested spectrometer	0.6%
The detecting system excursion and linearly of the untested spectrometer	0.5%
The stray light uncertainty	0.3%
Total uncertainty	2.6 %

**Table 6.** The uncertainty of the standard light irradiance calibration method

The irradiance uncertainty of the standard light F528 is provided by the NIST calibration report.

So the uncertainty of the lamp F528 calibrating the untested spectrometer with standard light method is 2.6%.

### 4.3. Two methods comparison

The irradiance responsivity of the untested spectrometer had been calibrated by the two methods. The calibration result is listed in the Table.7. Form the result we can see that the Standard detector calibration method has a higher accuracy comparing with the standard lamp calibration method. The calibration result comparison also approves the effectivity of the standard detector calibration method.

Wavelength	Irradiance response calibration of the untested spectrometer		Uncertainty comparison of the two calibration methods	
	Standard detector calibration result	Standard lamp calibration result	Standard detector calibration method	Standard lamp calibration method
nm	V.uw <sup>-1</sup> . cm <sup>2</sup> . nm	V.uw <sup>-1</sup> . cm <sup>2</sup> . nm		
313	4.80E+00	4.73E+00	1.90%	2.60%
352	5.67E+00	5.58E+00		
365	5.82E+00	5.72E+00		

**Table 7.** Irradiance response calibration result comparison between the two calibration methods

## 5. Conclusion

This paper introduces the standard detector calibration method. The detector standard source and standard transmission process is also discussed. And the HAUVSR is established using NIST standard detector. After a series of testing, the performance of the HAUVSR has been proved. We also deduce the responsivity standard of the HAUVSR, and its uncertainty is so high (1.3%). Using the HAUVSR, we calibrate the untested spectrometer with standard detector method. The calibration result is compared with the standard light calibration method. The comparison data indicates that the standard detector method can increase the calibration accuracy. The uncertainty of the standard detector calibration method (1.9%) is higher than the standard light calibration method (2.6%). Using this method, we can provide a untested sensor calibration result with higher accuracy. So our research on the standard calibration method is very important for the developing of the radiant calibration field.

## Author details

Wang Rui, Wang Tingfeng, Sun Tao, Chen Fei and Guo Jin  
*Changchun Institute of Optics, Fine Mechanics and Physics, Chinese Academy of Sciences,  
 State Key Laboratory of Laser Interaction with Matter, China*

## 6. References

- [1] D. F. Heath, A. J. Krueger, H. A. Roeder and B. D. Henderson. The Solar Backscatter Ultraviolet and Total Ozone Mapping Spectrometer (SBUV/TOMS) for NIMBUSG [J]. *Optical Engineering*, 1975, 14(4):323-331.
- [2] T.J.Quinn. Primary methods of measurement an primary standards [J].*Metrologia*.1997,20: 34-63.
- [3] F. Lei and J. Fischer, Characterization of Photodiodes in the UV and Visible Spectral Region-Based on Cryogenic Radiometry, *Metrologia* 30 (4), 297-303 (1993).
- [4] R. Goebel, R. Pello, R. Kohler, P. Haycocks, and N. P. Fox, Comparison of the BIPM Cryogenic radiometer with a mechanically cooled cryogenic radiometer from the NPL, *Metrologia* 33 (2), 177-179 (1996).
- [5] R. Kohler, R. Goebel, R. Pello, O. Touayar, and J. Bastie, First results of measurements with the BIPM cryogenic radiometer and comparison with the INM cryogenic radiometer, *Metrologia* 32 (6), 551-555 (1996).
- [6] R. Goebel, R. Pello, K. D. Stock, and H. Hofer, Direct comparison of cryogenic radiometers from the BIPM and the PTB, *Metrologia* 34 (3), 257-259 (1997).
- [7] J. E. Martin, N. P. Fox, and P. J. Key, A cryogenic radiometer for absolute radiometric measurements, *Metrologia* 21 147-155 (1985).
- [8] L. P. Boivin and K. Gibb, Monochromator-based cryogenic radiometry at the NRC, *Metrologia* 32 (6), 565-570 (1996).

- [9] J. M. Houston and J. P. Rice, NIST reference cryogenic radiometer designed for versatile performance, *Metrologia* 43 (2), S31-S35 (2006).
- [10] S. W. Brown, G. P. Eppeldauer, and K. R. Lykke, Facility for spectral irradiance and radiance responsivity calibrations using uniform sources, *Applied Optics* 45 (32), 8218-8237 (2006).
- [11] T. C. Larason, S. S. Bruce, and C. L. Cromer, The NIST high accuracy scale for absolute spectral response from 406 nm to 920 nm, *Journal of Research of the National Institute of Standards and Technology* 101 (2), 133-140 (1996).
- [12] T. R. Gentile, J. M. Houston, and C. L. Cromer, Realization of a scale of absolute spectral response using the national institute of standards and technology high-accuracy cryogenic radiometer, *Applied Optics* 35 (22), 4392-4403 (1996).
- [13] A. C. Parr, A National Measurement System for Radiometry, Photometry, and Pyrometry Based Upon Absolute Detectors, NIST Technical Note 1421 (1996).
- [14] T. C. Larason, S. S. Bruce, and A. C. Parr, Spectroradiometric detector measurements: part I-ultraviolet detectors and part II-visible to near-infrared detectors, NIST Special Publications 250-41, U.S. Government Printing Office, Washington, DC (1998).
- [15] P. S. Shaw, K. R. Lykke, R. Gupta, T. R. O'brian, U. Arp, H. H. White, T. B. Lucatorto, J. L. Dehmer, and A. C. Parr, Ultraviolet radiometry with synchrotron radiation and cryogenic radiometry, *Applied Optics* 38 (1), 18-28 (1999).
- [16] P. S. Shaw, T. C. Larason, R. Gupta, S. W. Brown, R. E. Vest, and K. R. Lykke, The new ultraviolet spectral responsivity scale based on cryogenic radiometry at Synchrotron Ultraviolet Radiation Facility III, *Review of Scientific Instruments* 72 (5), 2242-2247 (2001).
- [17] Donald.F.Heath, Zongying Wei, et al. Calibration and characterization of remote sensing instruments using ultra stable interference filters[J]. *SPIE*, 1997, 3221:300-308.
- [18] D.F. Heath, E. Hilsenrath, and S. Janz, Characterization of a 'hardened' ultra-stable UV linear variable filter and recent results on the radiometric stability of narrow band interference filters subjected to temperature/humidity, thermal/vacuum and ionizing radiation environments [J].*SPIE*, 1998, 3501: 410-421.
- [19] M.Durak,F.Samadov. Realization of a filter radiometer-based irradiance scale with high accuracy in the region from 286nm to 901nm[J].*Metrologia*,2004,41:401-406.
- [20] T.R.Gentile, J.M.Houston, J.E.Hardis, C.L.Cromer, A.C.Parr. National Institute of Standards and Technology high-accuracy cryogenic radiometer [J]. *Appl.Opt*, 1996, 35(7): 1056-1068.
- [21] Donald F,Heath, Zia Ahmad, Multipurpose spectroradiometer for satellite instrument calibration and zenith sky remote sensing measurements[J].*SPIE*,2001, 4150(45):115-123.

- [22] D.Einfeld, D.stuck and B.Wende. Calibration of radiometric transfer standards in the UV and VUV by electron synchrotron radiation using a normal incidence radiometer [J], Metrologia 1978, 14: 111-122.

IntechOpen

IntechOpen